Int. J. Electrochem. Sci., 11 **(2016)** 6183 – 6191, doi: 10.20964/2016.07.05

International Journal of
ELECTROCHEMICAL
SCIENCE
www.electrochemsci.org

Electrodeposition of Tin Based Film on Copper Plate for Electrocatalytic Reduction of Carbon Dioxide to Formate

Weixin Lv, Jing Zhou, Jingjing Bei, Rui Zhang[*]*, Fenying Kong, Wei Wang*[*]

School of Chemistry and Chemical Engineering, Yancheng Institute of Technology, Yancheng 224051, China
[*]E-mail: zhangrui20128@163.com, wangw@ycit.edu.cn

Received: 29 March 2016 / *Accepted:* 5 May 2016 / *Published:* 4 June 2016

Sn based film with a thickness of 169 nm has been electrodeposited on copper plate from a choline chloride/ethylene glycol based electrolyte containing $SnCl_2$. Electrochemical reduction of carbon dioxide (CO_2) has been studied on the prepared Sn based film electrode in $KHCO_3$ aqueous solution. The electrolysis results show that the faradaic efficiency for producing formate is affected by the time of the electrode exposed to air and the electrolysis potential. We find that the Sn based film can improve the electrocatalytic activity for CO_2 reduction. The faradaic efficiency for producing formate on the Sn based film electrode (74.1%) is higher than that on the Cu plate electrode.

Keywords: Electrodeposition; Tin based film; Carbon dioxide; Electrocatalytic reduction; Formate

1. INTRODUCTION

Current energy production methods raise atmospheric concentrations of CO_2, which is the key factor for climate change because of its greenhouse properties. Recycling and converting CO_2 into useful fuels and chemical feedstocks have become a significant challenge [1-4]. Among the several pathways to reduce CO_2 concentration, electrochemical reduction of CO_2 has received considerable interest as it consumes less energy than traditional chemical reduction processes and can operate benignly under ambient reaction conditions [5-10].

Among various available products from electrochemical reduction of CO_2, formic acid/formate is one of the highest value-added chemicals. Formic acid is widely used in the textile industry, tanning industry, rubber processing industry, and pharmaceutical industry [11]. Formic acid could also function as an energy vector for the storage of excess of electricity, as it can be used in the direct formic acid fuel cell to produce electricity [12]. Electrochemical reduction of CO_2 to formate as a large

scale application is economically feasible which were announced by many researchers, and the economic feasibility of this process depends intensely on the cathode material, including its electrochemical performance and cost [6]. Dominguez-Ramos et al. investigated the environmental sustainability of producing formate or formic acid by electrochemical reduction of CO_2, and found that the greenhouse gas emission for the process was 0.33 kg CO_2 for producing 1 kg of $HCOO^-$ under the optimistic conditions, which was lower than the current commercial production processes (3.1 kg CO_2) [13]. Agarwal et al. also discussed the engineering and economic feasibility of large scale electrochemical reduction of CO_2 to formate, and suggested that this process can be operationally profitable [14].

The success of electrochemical reduction of CO_2 to formate hinges on the development of efficient electrocatalysts that selectively and efficiently reduce CO_2 using H_2O as an H^+ source. One of the fundamental challenges in catalyst development is to suppress the reduction of H^+ to H_2 [15, 16]. Metal electrodes were commly used for the study of electrochemical reduction of CO_2, and most of them have a strong preference for H^+ reduction over CO_2 reduction in aqueous solutions [17]. Unlike other metals, the metals with high hydrogen overpotentials, such as Sn, Bi, Pb, In and Hg, tend to produce formate in aqueous solutions with high selectivity and high faradaic efficiency [5, 17-23]. Chen et al. prepared a thin-film catalyst by simultaneous electrodeposition of Sn^0 and SnO_x on a Ti electrode, which exhibited up to 4-fold higher faradaic efficiency for CO_2 reduction than a Sn electrode with a native SnO_x layer [24]. Kwon et al. prepared three-dimensional active Pb electrodes on Pt substrate by applying stepwise potential deposition, and they observed higher faradaic efficiency of this electrode (94.1%) than that of commercial Pb foil (52.3%) at 5 °C [25]. These researches indicated that the electrodeposition metal catalyst on the substrate can be used as the electrode for electrochemical reduction of CO_2.

In this paper, a Sn based film was prepared on Cu plate substrate by electrochemical deposition in nonaqueous solution, which was used as cathode for electrochemical reduction of CO_2. The influences of key variables like the time of the electrode exposed to air and the electrolysis potential on electrochemical reduction of CO_2 to formate were studied to obtain the optimal electrolysis conditions.

2. EXPERIMENTAL

2.1. Preparation of Sn/Cu electrode

A Cu plate (0.1 mm thick) was ultrasonically cleaned with ethanol and deionized water, dried with flowing air and electropolished in 85% H_3PO_4 at 4 V vs. a Pt counter electrode for 5 min, successively. Then the obtained Cu plate was used as the substrate for electrochemical deposition of Sn. The electrochemical deposition was performed on the Cu substrate in nonaqueous solution containing 0.1 mol L^{-1} $SnCl_2$. The nonaqueous solution was formed by stirring choline chloride and ethylene glycol in a mol ratio of 1:2 at 80 °C for about 30 min. Sn based film was deposited on the Cu substrate by electrochemical deposition at 0.7 V for 5 min, and the sample was marked as Sn/Cu electrode.

2.2. Electrochemical experiments

The electrochemical experiments were carried out using a conventional three-electrode system in an airtight and undivided glass cell equipped with a gas inlet and outlet which is able to pass either N_2 (99.99%) or CO_2 (99.99%) through the solution. The working electrode was the prepared Sn/Cu electrode with the geometric surface area of 1 cm^2. A Pt plate (2 cm^2) and an Ag/AgCl electrode (sat. KCl) was chosen as the counter electrode and the reference electrode. All potential values are in reference to Ag/AgCl electrode. The electrolyte used was 40 mL of 0.1 mol L^{-1} $KHCO_3$ aqueous solution. All experiments were performed under room temperature (22 ± 3 °C) and ambient pressure.

The electrochemical measurements were performed with a CHI 660D electrochemical workstation (Shanghai Chenhua Instruments Co., Ltd., China). Linear sweep voltammetry (LSV) was performed in 0.1 mol L^{-1} $KHCO_3$ aqueous solution after being bubbled with N_2 or CO_2 for 30 min at a scan rate of 0.05 V s^{-1}. The current density (j) is determined on the geometrical area of the electrode.

Electrolysis was carried out potentiostatically using a LAND CT2001C cell performance-testing instrument (Wuhan Electronics Co., Ltd., China). The electrolyte was saturated with CO_2 before each electrolysis process, and CO_2 gas was bubbled continuously at a flow rate of 20 mL min^{-1} during the electrolysis process. The electrolysis experiments were terminated when the amount of charge passed reached to 50 C. The average current density (j_a) is expressed as the total current divided by the geometric area of the electrode.

2.3. Analysis and calculations

Scanning electron microscope (SEM) images were collected by a Hitachi S-4800 microscope at an acceleration voltage of 15 kV. X-ray diffraction pattern (XRD) was recorded on a Rigaku D/MAX 2200 diffractometer using Cu Kα radiation (λ = 1.54056 Å), scan range from 25 to 80 ° at a scan rate of 0.12 ° s^{-1}.

The products in the electrolyte after electrolysis were directly analyzed by ion chromatography (ICS-900 Dionex). The column was an IonPac AS11-HC anionic column using 0.02 mol L^{-1} KOH as the mobile phase at the rate of 1 mL min^{-1}. 10 μL of the electrolyte were used for each time.

The faradaic efficiency for pruducing formate (f) is determined by equation (1):

$$f = 2nF / Q \quad (1)$$

where 2 represents two electrons required for the formation of one molecule of formate from CO_2; n is the moles of the formate produced which can be calculated according to the data of ion chromatography; F is Faraday's constant (96485 C mol^{-1} of electrons); and Q is the total charge passed across the electrode during the electrolysis process (Q = 50 C here).

3. RESULTS AND DISCUSSION

Fig. 1a and b give the morphologies of the Cu plate before and after electropolishing, from which it can be seen that the surface of the Cu substrate is smooth after electropolishing. It also can be

seen from the inset of Fig. 1b that there has no impurity on the surface of the Cu substrate after electropolishing. Fig. 1c gives the morphology of the Sn based film on the Sn/Cu electrode, which shows that the Sn based film is tightly adhered to the Cu substrate. Fig. 1d shows the EDS spectrum of the Sn/Cu electrode. It can be seen that the peaks of Sn appear obviously and the atomic percents of Sn and Cu are 14.5% and 85.5%. The results from Fig. 1c and d indicate that Sn has been deposited on the Cu substrate successfully. The thickness of Sn based film (δ) on the Sn/Cu electrode is around 169 nm thick, which can be roughly calculated by equation (2):

$$\delta = (m_2 - m_1) \times 10^7 / (\rho S) \quad (2)$$

where m_1 and m_2 are the weights of the Cu plate substrates before and after electrodeposition of Sn, respectively, and the units of which are gram; ρ is the density of Sn (7.298 g cm^{-3}); S is the geometric surface area of the Cu plate substrate (S = 10 cm^2 here).

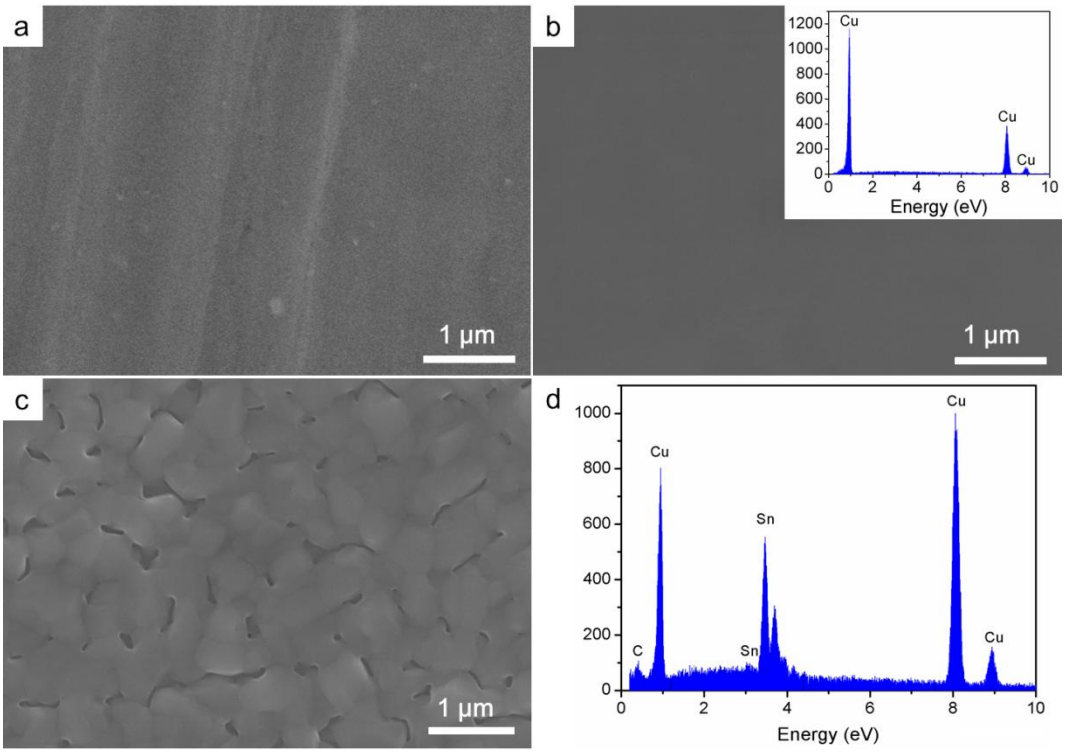

Figure 1. (a-c) SEM pictures of the Cu plate (a), the polished Cu plate (the inset is its EDS spectrum) (b), and the Sn/Cu electrode (c). (d) EDS spectrum of the Sn/Cu electrode.

Fig. 2 gives the XRD pattern of the Sn/Cu electrode. The peaks at 43.3, 50.4, and 74.1 ° are assigned to (111), (200), and (220) planes of the Cu substrate (PDF 4-836), respectively. Other peaks should be attributed to the Sn based film, which indicates the presence of two basic phases in Sn based film: Sn (PDF 1-926) and Cu_3Sn (PDF 65-4653). The peaks at 30.7, 32.1, and 64.2 ° are assigned to (200), (101), and (400) planes of the deposited Sn, respectively, and the peak at 77.3 ° is assigned to (103) plane of Cu_3Sn. The in situ formation of Cu_3Sn layer can be attributed to the mutual diffusion of the Sn and Cu atoms [26].

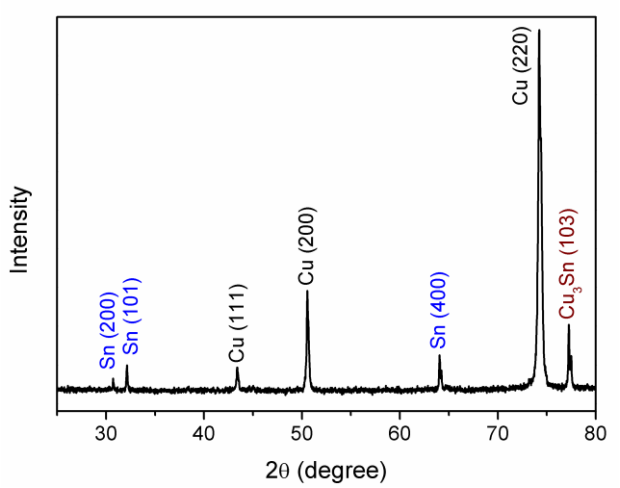

Figure 2. XRD pattern of the Sn/Cu electrode.

In this experiment, we found that the exposure time of the Sn/Cu electrode in the air will affect its electrochemical behavior, so we compared the electrochemical behaviors of the Sn/Cu electrodes exposed to air for 0 and 24 h. Fig. 3 depicts the LSV curves of the Sn/Cu electrodes in 0.1 mol L^{-1} $KHCO_3$ solutions after being bubbled with N_2 or CO_2 for 30 min. As shown in Fig. 3, under CO_2, the current density of the Sn/Cu electrode exposed to air for 0 h is a little higher than that exposed to air for 24 h; whereas under N_2, it is greatly higher than that exposed to air for 24 h. Under N_2, this increase is due to the H_2 evolution only; under CO_2, the enhanced current must be caused by both the reduction of the CO_2 and the evolution of H_2. The LSV results illustrate that the seriously H_2 evolution reaction causes the CO_2 reduction activity of the Sn/Cu electrode exposed to air for 0 h decrease. The electrolysis experiments were also carried out at −1.8 V in CO_2 saturated 0.1 mol L^{-1} $KHCO_3$ aqueous solution, which is the optimal electrolysis condition abtained by our previous work [27].

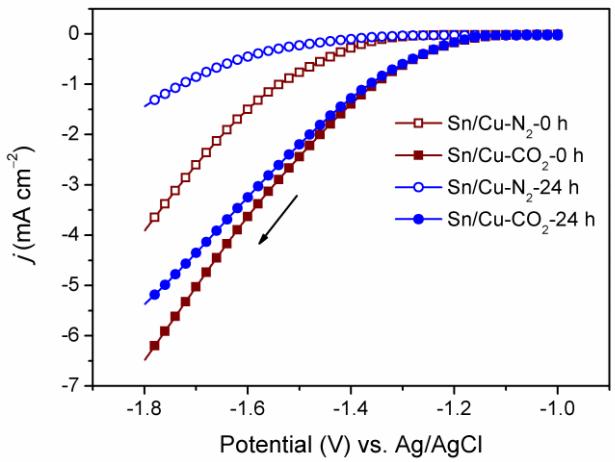

Figure 3. LSV curves on the Sn/Cu electrodes exposed to air for 0 and 24 h before the LSV measurements, respectively. The measurements were carried out in 0.1 mol L^{-1} $KHCO_3$ solution after being bubbled with N_2 (hollow) and CO_2 (solid) for 30 min at a scan rate of 0.05 V s^{-1}.

The faradaic efficiency for producing formate of the Sn/Cu electrode exposed to air for 0 h is 41.3%; and when the exposure time is 24 h, the faradaic efficiency can reach to 74.1%.

It is known that when the Sn/Cu electrode is exposed to air, the surface of Sn based film will be oxidized slowly. Chen et al. compared the faradaic efficiency for producing formate on the Sn electrode without oxide layer to that on the SnO_x/Sn electrode at low electrolysis potential (−1.14 ~ −1.34 V vs. Ag/AgCl), and found that the faradaic efficiency of the Sn electrode without oxide layer was lower than 1%, whereas that of the SnO_x/Sn electrode was up to 40% [24]. Zhang et al. revealed that the H_2 evolution reaction is more likely to happen on the Sn electrode without oxide layer, and the oxide layer of the Sn electrode can inhibits the H_2 evolution reaction [28]. If the Sn electrode without oxide layer is exposed to the air, its surface will be oxidized gradually. It indicates that for the Sn/Cu electrode exposed to air for 24 h, its oxide layer inhibits the competing reaction (H_2 evolution reaction) of CO_2 reduction reaction, therefore it exhibits high activity for CO_2 reduction. Consequently, the Sn/Cu electrodes were exposed to air for 24 h in the following experiments.

The effects of electrolysis potential on the faradaic efficiency and the average current density for producing formate during the electrochemical reduction of CO_2 have been investigated, and the results are shown in Fig. 4. It can be seen that the average current density increases as the electrolysis potential decreases from −1.5 to −1.9 V. The faradaic efficiency for producing formate increases as the electrolysis potential decreases from −1.5 to −1.8 V, and reaches to the maximum (74.1%) at −1.8 V. As the electrolysis potential decreases further, the faradaic efficiency begins to decrease. These results are consistent with other literatures of the Sn electrode [19, 28].

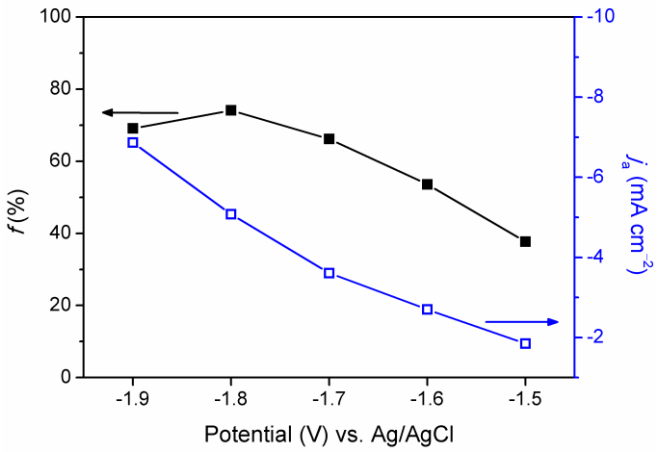

Figure 4. Variations of the faradaic efficiency (■) and the average current density (□) for producing formate with the electrolysis potential.

Fig. 5 shows the variations of the electrolysis current density with the electrolysis time during the electrochemical reduction of CO_2 at different electrolysis potentials. It can be seen that the current density remains almost un-changed at each electrolysis potential, which may mean that the Sn/Cu electrode as the cathode exhibits stable performance [29]. It also can be seen that the lower the electrolysis potential is, the stronger the electrolysis current density vibrates, this can be attributed to

the enhancement of H_2 evolution at more negative electrolysis potentials. We can see that bubbles form and increase fast on the surface of the Sn/Cu cathode at more negative electrolysis potentials during the electrolysis process.

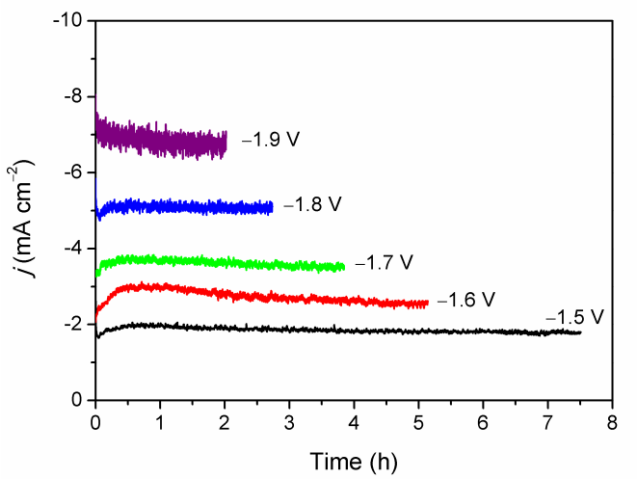

Figure 5. Variations of the electrolysis current density with electrolysis time during the electrochemical reduction of CO_2 at the electrolysis potentials from −1.5 to −1.9 V.

Fig. 6 depicts the LSV curves of the polished Cu plate electrode and the Sn/Cu electrode in 0.1 mol L^{-1} $KHCO_3$ solutions after being bubbled with N_2 or CO_2 for 30 min. For the Sn/Cu electrode, the reduction current density under CO_2 is the biggest, and that under N_2 is the smallest. Under N_2, the increase of the current is due to the reduction of H_2O (H_2 evolution reaction) only; under CO_2, the enhanced current must be caused by the reduction of both H_2O and CO_2 [3]. It indicates that the Sn/Cu electrode has excellent electrocatalytic activity toward CO_2 reduction.

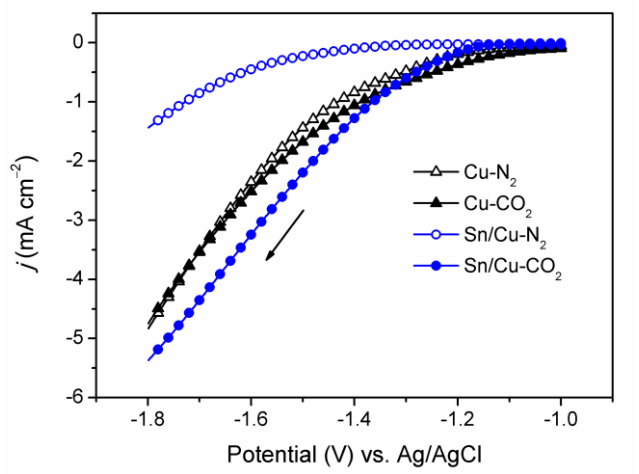

Figure 6. LSV curves on the polished Cu electrode and the Sn/Cu electrode in 0.1 mol L^{-1} $KHCO_3$ solutions after being bubbled with N_2 (hollow) and CO_2 (solid) for 30 min at a scan rate of 0.05 V s^{-1}.

We also carried out the electrolysis experiments on the polished Cu plate electrode at −1.8 V in CO_2 saturated 0.1 mol L^{-1} $KHCO_3$ solution, the electrolysis results are shown in Fig. 7. It can be found that, for the polished Cu electrode and the Sn/f-Cu electrode, the faradaic efficiencies for producing formate are 20.2% and 74.1%, respectively; the average current densities for electrolysis are 5.69 and 5.08 mA cm^{-2}, respectively; the production rates for electrochemical reduction of CO_2 to formate are 21.4 and 70.3 μmol h^{-1}, respectively. For the polished Cu electrode, the average current density is high, whereas the faradaic efficiency and the production rate of formate are great lower than those of the Sn/Cu electrode. It is well known that the faradaic efficiency for producing formate on Cu electrode is very low [30, 31]. The above results demonstrate that depositon a layer of Sn based film can improve the electrocatalytic activity of Cu electrode toward CO_2 reduction. It can be concluded that the Sn/Cu electrode is an excellent electrode for electrochemical reduction of CO_2 to formate.

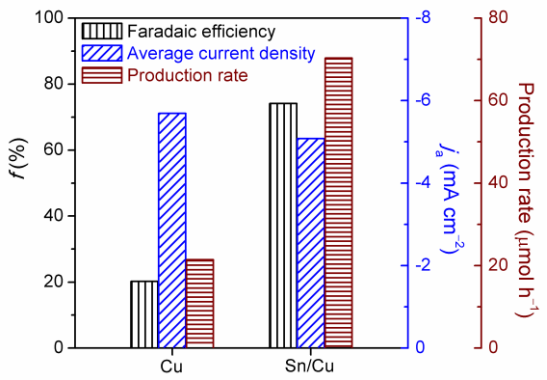

Figure 7. Faradaic efficiencies, average current densities and production rates for electrochemical reduction of CO_2 to formate on the polished Cu electrode and the Sn/f-Cu electrode.

4. CONCLUSIONS

Sn/Cu electrode has been prepared by deposition a Sn based film on Cu plate substrate, which has been used as cathode for electrocatalytic reduction of CO_2 to formate. Faradaic efficiency for producing formate is influenced by the time of the Sn/Cu electrode exposed to air and the electrolysis potential. The Sn/Cu electrode exposed to air for 24 h shows better preformance for CO_2 reduction, because the Sn film surface can be gradually oxidized and form an oxide layer which can inhibit the competing reaction (H_2 evolution reaction) of CO_2 reduction reaction.

When the electrolysis is carried out at the optimum conditions, that is, the electrolysis is carried out at −1.8 V vs. Ag/AgCl on the Sn/Cu electrode exposed to air for 24 h, the faradaic efficiency for producing formate can reach to 74.1%.

ACKNOWLEDGEMENTS
This work was supported by the joint research fund between Collaborative Innovation Center for Ecological Building Materials and Environmental Protection Equipments and Key Laboratory for Advanced Technology in Environmental Protection of Jiangsu Province, the National Natural Science Foundation of China (21305122), the Natural Science Foundation of Jiangsu Province (BK20131218)

and the Industry-University-Research Cooperative Innovation Foundation of Jiangsu Province (BY2014108-08).

References

1. J. Medina-Ramos, J. L. DiMeglio and J. Rosenthal, *J. Am. Chem. Soc.*, 136 (2014) 8361
2. Y. Oh and X.L. Hu, *Chem. Soc. Rev.*, 42 (2013) 2253
3. W. X. Lv, J. Zhou, F. Y. Kong, H. L. Fang and W. Wang, *Int. J. Hydrogen Energ.*, 41 (2016) 1585
4. C. Riplinger, M. D. Sampson, A. M. Ritzmann, C. P. Kubiak and E. A. Carter, *J. Am. Chem. Soc.*, 136 (2014) 16285
5. H. Z. Zhao, Y. Zhang, Y. Y. Chang and Z. S. Li, *J. Power Sources*, 217 (2012) 59
6. Q. N. Wang, H. Dong and H. B. Yu, *RSC Adv.*, 4 (2014) 59970
7. F. Zhou, S. M. Liu, B. Q. Yang, P. X. Wang, A. S. Alshammari and Y. Q. Deng, *Electrochem. Commun.*, 46 (2014) 103
8. S. Zhang, P. Kang, S. Ubnoske, M. K. Brennaman, N. Song, R. L. House, J. T. Glass and T. J. Meyer, *J. Am. Chem. Soc.*, 136 (2014) 7845
9. J. Shi, F. Shi, N. Song, J. X. Liu, X. K. Yang, Y. J. Jia, Z. W. Xiao and P. Du, *J. Power Sources*, 259 (2014) 50
10. J. L. Qiao, Y. Y. Liu, F. Hong and J. J. Zhang, *Chem. Soc. Rev.*, 43 (2014) 631
11. H. Uslu, C. Bayat, S. Goekmen and Y. Yorulmaz, *J. Chem. Eng. Data*, 54 (2009) 48
12. J. Yang, C. G. Tian, L. Wang and H. G. Fu, *J. Mater. Chem.*, 21 (2011) 3384
13. A. Dominguez-Ramos, B. Singh, X. Zhang, E .G. Hertwich and A. Irabien, *J. Clean. Prod.*, 104 (2015) 148
14. A. S. Agarwal, Y. M. Zhai, D. Hill and N. Sridhar, *ChemSusChem*, 4 (2011) 1301
15. S. Zhang, P. Kang and T. J. Meyer, *J. Am. Chem. Soc.*, 136 (2014) 1734
16. Y. C. Lan, S. C. Ma, P. J. A. Kenis and J. X. Lu, *Int. J. Electrochem. Sci.*, 9 (2014) 8097
17. H. Noda, S. Ikeda, Y. Oda, K. Imai, M. Maeda and K. Ito, *Bull. Chem. Soc. Jpn.*, 63 (1990) 2459
18. R. Zhang, W. X. Lv, G. H. Li, M. A. Mezaal, X. J. Li and L. X. Lei, *J. Power Sources*, 272 (2014) 303
19. G. K. S. Prakash, F. A. Viva and G. A. Olah, *J. Power Sources*, 223 (2013) 68
20. J. J. Wu, P. P. Sharma, B. H. Harris and X. D. Zhou, *J. Power Sources*, 258 (2014) 189
21. D. T. Whipple and P. J. A. Kenis, *J. Phys. Chem. Lett.*, 1 (2010) 3451
22. Q. N. Wang, H. Dong, H. Yu and H. B. Yu, *J. Power Sources*, 279 (2015) 1
23. M. F. Baruch, J. Pander, J. L. White and A. B. Bocarsly, *ACS Catal.*, 5 (2015) 3148
24. Y. H. Chen and M. W. Kanan, *J. Am. Chem. Soc.*, 134 (2012) 1986
25. Y. Kwon and J. Lee, *Electrocatalysis*, 1 (2010) 108
26. C. D. Gu, Y. J. Mai, J. P. Zhou, Y. H. You and J. P. Tu, *J. Power Sources*, 214 (2012) 200
27. W. X. Lv, R. Zhang, P. R. Gao and L. X. Lei, *J. Power Sources*, 253 (2014) 276
28. R. Zhang, W. X. Lv and L. X. Lei, *Appl. Surf. Sci.*, 356 (2015) 24
29. J. J. Wu, F. G. Risalvato, F. S. Ke, P. J. Pellechia and X. D. Zhou, *J. Electrochem. Soc.*, 159 (2012) F353
30. Y. Hori, H. Wakebe, T. Tsukamoto and O. Koga, *Electrochim. Acta*, 39 (1994) 1833
31. S. Sen, D. Liu and G. T. R. Palmore, *ACS Catal.*, 4 (2014) 3091